coatings

MDPI

Article

Assessment on the Effects of ZnO and Coated ZnO Particles on iPP and PLA Properties for Application in Food Packaging

Antonella Marra *, Gennaro Rollo, Sossio Cimmino and Clara Silvestre

Institute of Polymers, Composites and Biomaterials (IPCB), Consiglio Nazionale delle Ricerche (CNR), Via Campi Flegrei 34, Pozzuoli (Na) 80078, Italy; gennaro.rollo@ipcb.cnr.it (G.R.); sossio.cimmino@ipcb.cnr.it (S.C.); clara.silvestre@ipcb.cnr.it (C.S.)

* Correspondence: antonella.marra@ipcb.cnr.it; Tel.: +39-081-867-5203; Fax: +39-081-867-5230

Academic Editor: Stefano Farris

Received: 15 November 2016; Accepted: 8 February 2017; Published: 17 February 2017

Abstract: This paper compares the properties of iPP based composites and PLA based biocomposites using 5% of ZnO particles or ZnO particles coated with stearic acid as filler. In particular, the effect of coating on the UV stability, thermostability, mechanical, barrier, and antibacterial properties of the polymer matrix were compared and related to the dispersion and distribution of the loads in the polymer matrix and the strength of the adhesion between the matrix and the particles. This survey demonstrated that, among the reported systems, iPP/5%ZnOc and PLA/5%ZnO films are the most suitable active materials for potential application in the active food packaging field.

Keywords: isotactic polypropylene; polylactic acid; zinc oxide; stearic acid; properties; composites; antibacterial activity; active food packaging

1. Introduction

Nano- and micro-technologies are applicable in food packaging to improve packaging performance such as gas, moisture, UV and volatile barriers, mechanical strength, heat resistance, flame retardancy, etc. [1–7]. Application of these technologies in food packaging is, therefore, considered highly promising since these technologies could also improve safety and quality of food and the research is oriented not only to materials with increased mechanical properties and reduced permeability but also those having antimicrobial properties [8–17]. It has been shown that the use of active agents, incorporated in the polymeric material for packaging, increases the shelf-life of the packaged product (life duration of a foodstuff before its consumption), acting on those mechanisms of degradation that cause food deterioration and reducing/inhibiting the growth of pathogens [18–20]. Particles of metals and metal oxides at sub-micrometric and/or nanometric size are the most used particles to develop antimicrobial activity [21]. Silver particles are already found in many commercial products. In literature, it is reported that Ag exerts antibacterial and fungicidal effects on about 150 different types of bacteria when the metal particles have nanoscale size [22–25].

Among metal oxides, zinc oxide (ZnO) is known to act as an antibacterial agent in addition to its ability to block UV radiation [26]. Recent studies confirm the efficacy of ZnO particles as antimicrobial agents when used in thermoplastic polymers [27–30]. From these studies emerged important results: ZnO particles exhibit antimicrobial activity against bacteria that are resistant to high temperatures and pressures; the antibacterial activity is dependent on the surface area and concentration, while the crystalline structure and shape of the particles have little influence; the treatment of the ZnO particles at higher temperature has a significant effect on the antibacterial activity. Despite this, the mechanism of antimicrobial activity is not fully clarified: according to Sawai et al. [27], the formation of hydrogen

peroxide is able to destroy the cell membrane; according to Stoimenov et al. [31] ZnO particles link through chemical bonds to the bacterial membrane and cause the formation of electrostatic forces that damage the cell membrane itself. Anyway, the most creditable hypothesis is the formation of reactive oxygen species even if it is not yet entirely clear how these species are produced [32]. ZnO is currently listed as a generally recognized as safe (GRAS) material by the Food and Drug Administration and is used as food additive [33]. It must also be underlined that, for a complete application of these technologies, release of these particles from the packaging to food needs to be assessed in order to assure the safety of the new materials [6,34].

This paper reports the results obtained using 5% of ZnO particles and of ZnO particles coated (ZnOc) with stearic acid in order to modify the characteristics of two polymers, one derived by oil, isotactic polypropylene (iPP), and the other derived from renewable resources, polylactide acid (PLA), largely used in the field of food packaging [8–10,35–37]. Considering our previous studies [8–10], it is believed that 5% is the best amount to use, in order to improve the characteristics of composites, especially for the antibacterial properties. To have a complete pattern of the two systems additional analysis have been performed and unpublished results will be presented. In particular, we analyze how the distribution and dispersion of the ZnO particles, coated or not, and their adhesion to the two different matrices (iPP and PLA) affect the UV stability; thermostability; and mechanical, barrier, and antibacterial properties.

2. Experimental

2.1. Materials and Sample Preparation

The materials object of this assessment are: (1) isotactic polypropylene (iPP, Moplen X30S), in pellets, kindly supplied by Basell (Ferrara, Italy), with melt flow index = 9 dg·min^{-1} (2.16 kg, 230 °C), M_w = 3.5 × 10^5 and M_n = 4.7 × 10^4; (2) polylactic acid (PLA 4032D), in pellets, acquired from Nature Works LLC with d = 1.24 g/cm^3 and M_w = 2.1 × 10^5 (g/mol), M_n = 1.3 × 10^5 (g/mol), polydispersity = 1.6, M_w/M_n determined by GPC-150C Waters Chromatography instrument (Milford, MA, USA) GPC at IPCB-CNR; (3) Zinc oxide powder, (Pylote SAS, in Dremil-Lafage, France). The procedures to obtain and/or to coat the ZnO were reported in details in references [14,15,38–41]. In particular ZnO particles were synthesized using a preindustrial spray scale pyrolysis platform the Pylote in Toulouse, France, in order to have high purity of the obtained powders, more uniform chemical composition, narrow size distribution, better regularity in shape, and the ability to synthesize multicomponent materials [38–41]. The coating of the ZnO particles was performed by preparing a solution of stearic acid and ZnO (1:10) in isopropanol under stirring for 12 h. The final product contains 9% of stearic acid linked to the surface of the particles as evaluated through thermogravimetric analysis as reported in details in Silvestre et al. [10]. In this reference [10], it is also reported that the coating process does not alter the crystalline structure of the particles, whereas it causes an increase of the dimension of the particle (the size of the ZnO particles ranges between 250 to 500 nm while that of the particles of ZnOc varies between 1 to 1.2 μm), and a change in the shape of the particles (hexagonal for the uncoated particles to spherical shape in the case of ZnOc particles). The composites were produced in a twin-screw extruder, Collin ZK25 (Ebersberg, Germany) with the D = 25 mm and L/D = 56, at the following temperatures from the hopper to the die: 180/200/200/190/180 °C for iPP based composites, and 150/170/170/170/160 °C for PLA based composites; the speed of the extruder screws was 25 rpm. In this review, the properties of the following system will be compared: iPP; iPP/5%ZnO; iPP/5%ZnOc; PLA; PLA/5%ZnO; PLA/5%ZnOc.

2.2. Characterization Methodologies

2.2.1. Scanning Electron Microscopy (SEM)

The morphology of the fractured surfaces of the composites were determined by the scanning electron microscope (SEM). The model used is a Fei Quanta 200 SEM Feg, Hillsboro, OR, USA.

The scanning electron microscope is an instrument characterized by a high resolving power, of the order of 200–300 Å, and provides three-dimensional images of the surfaces observed. The samples were then fixed on a support and metallized with a gold-palladium alloy to ensure better conductivity and prevent the formation of electrostatic charges.

2.2.2. Antibacterial Activity

The antimicrobial activity of the biocomposites was evaluated by using *E. coli* DSM 498T (DSMZ, Braunschweig, Germany) as test microorganisms. The evaluation was performed using the ASTM Standard Test Method E 2149-10 preparation of the bacterial inoculum required to grow a fresh 18 h shake culture of *E. Coli* DSM 498 in a sterile nutrient broth (composition for 1 L: 10 g of tryptone, 5 g of yeast extract and 10 g of sodium chloride) [42]. The colonies were maintained according to good microbiological practice and examined for purity by creating a streak plate.

The bacterial inoculum was diluted using a sterile buffer solution (composition for one liter: 0.150 g of potassium chloride, 2.25 g of sodium chloride, 0.05 g of sodium bicarbonate, 0.12 g of calcium chloride hexahydrate and at pH = 7.0) until the solution reached an absorbance of 0.30 $\pm$ 0.01 at 600 nm, as measured spectrophotometrically. This solution, with concentration of 1.5×10^8–3.0×10^8 colony forming units (CFU/mL), was diluted with the buffer solution to obtain a final concentration of 1.5×10^6–3.0×10^6 CFU/mL and it was the working bacterial dilution. The experiments were performed in 50 mL sterilized flasks. One gram of the film was maintained in contact with 10 mL of the working bacterial dilution. After 2 min, 100 mL of the working bacterial dilution was transferred to a test tube, which was followed by serial dilution and plating out on Petri dishes (10 mm $\times$ 90 mm) in which the culture media was previously poured. The Petri dishes were incubated at 35 °C for 24 h. These dishes represented the T_0 contact time. The flasks were then placed on a wrist-action shaker for 0 h and 48 h. The bacterial concentration in the solutions at these two fixed times was evaluated by performing again serial dilutions and standard plate counting techniques. Three experiments were performed for each composition. The number of colonies in the Petri dish after incubation was converted into the number of colonies that form a unit per milliliter (CFU/mL). The percentage reduction was calculated using the following formula:

$$\% \text{ Reduction (CFU/mL)} = [(B-A)/B] \times 100 \quad (1)$$

where A = CFU/mL for the flask containing the sample after the specific contact time and B = CFU/mL at T_0.

2.2.3. UV-Visible Spectrophotometry

UV-Visible spectra were monitored with Jasco V-570 spectrophotometer, Columbia, MA, USA. The spectra were recorded by using films in transmission mode.

2.2.4. Thermogravimetric Analysis (TGA)

The thermal stability of the samples was studied by TGA. The instrument used was a Perkin Elmer Diamond, Massachusetts, USA. Thermogravimetry consists in recording the variation of mass of a sample as a function of time and/or temperature in a controlled atmosphere.

The measurements were conducted at a heating rate of 20 °C/min from 30 to 800 °C, using about 1.5/2.0 mg of the sample in alumina pan. The experiments were done in an oxygen atmosphere at flow rate of 200 mL/min. From thermograms it is determined that the temperature at which the degradation process is at 50%.

2.2.5. Mechanical Properties (Tensile)

The tensile properties were determined by using a dynamometer Instron 4505, Torino, Italy, with appropriate software for data processing. The tests were carried out at ambient temperature and at a speed of the moving crosshead of 2 mm/min. At least 20 tests were performed for each film composition.

2.2.6. Percentage Variation of Oxygen Permeability

The apparatus used is Permeo$_2$ Extra Solution Instrument, Lucca, Italy. The test consists in determining the amount of oxygen that passes through the surface (50 cm^2) of the film, in 24 h, with precise relative humidity condition H = 0% and temperature at 23 °C.

The permeability is obtained, multiplying the Oxygen Transmission Rate (OTR) [cm^3/(m^2 × 24 h)], obtained by the measurement, for the film thickness (cm) and dividing by the difference of partial pressure (bar) present in the two chambers

$$\text{Permeability} = \text{OTR} \times (\text{thickness}/\Delta P) = [\text{cm}^3/(\text{m}^2 \times 24\ \text{h})] \times (\text{cm/bar}) \quad (2)$$

The percentage variation of O_2 permeability of composite systems, ΔO_2 Permeability (%), is calculated using the following formula:

$$\Delta O_2\ \text{Permeability}\ (\%) = [(P_c - P_p)/P_p] \times 100 \quad (3)$$

where P_c is the oxygen permeability of the composite film and P_p is the oxygen permeability of the plain film.

3. Results and Discussion

3.1. Overall Morphology

For the systems under examination, the dispersion of the particles on the polymeric matrix depends on the coating process and on the kind of matrix used. Figure 1 shows the SEM images of all systems composites based on iPP and PLA matrix.

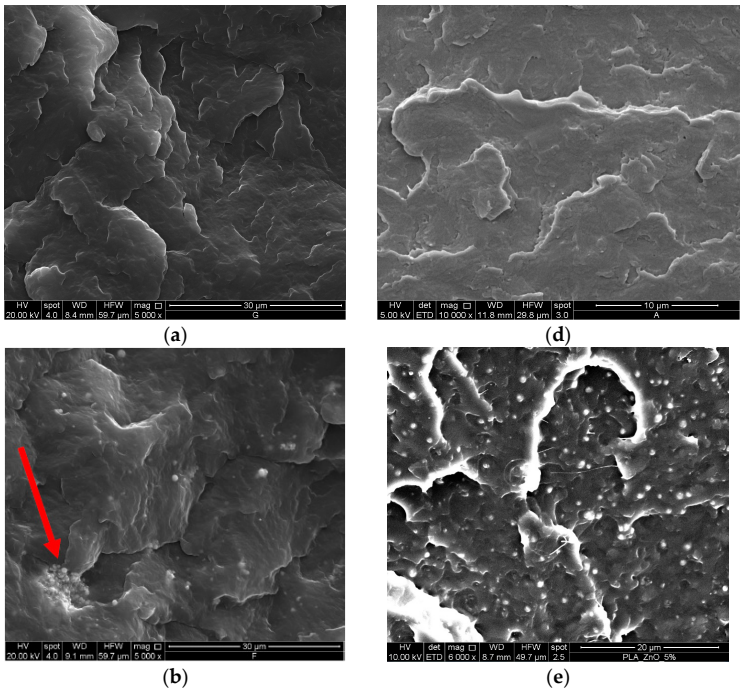

(**a**) (**d**)

(**b**) (**e**)

Figure 1. *Cont.*

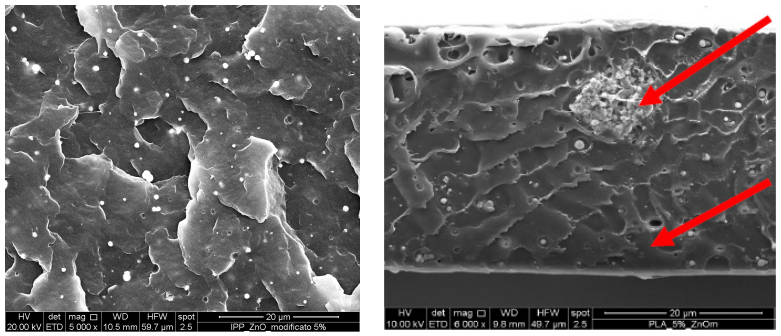

Figure 1. Scanning electron micrographs of iPP (**a**), iPP/ZnO (**b**), iPP/ZnOc (**c**), PLA (**d**), PLA/ZnO (**e**), and PLA/ZnOc (**f**) films fractured in liquid nitrogen.

The iPP/ZnO samples are characterized by a not homogeneous distribution of the particles with the presence of agglomerates, Figure 1b. It should be noted that the ZnO particles are well embedded in the iPP matrix. For the iPP system, the coating of the ZnO with stearic acid (Figure 1c) promotes a better dispersion and distribution of the particles and prevents the formation of agglomerates [10]. Using the same particles, in PLA matrix it is possible to note an opposite behavior: whereas for the system PLA/ZnO, Figure 1e, the distribution of the uncoated particles in the sample is homogenous, with the particles well embedded in the matrix, for the PLA/ZnOc system, Figure 1f, agglomerations of particles are present. Moreover, the presence of holes left during the fracture with liquid nitrogen indicates a poor adhesion between matrix and particles.

3.2. Antibacterial Activity

In Figure 2, the antimicrobial effect against *E. coli* is presented for iPP and PLA based systems. Plain polymers exhibit no bactericidal activity. When ZnO or ZnOc particles are present in both matrices after 48 h the composites show a reduction of 99.99% of *E. coli*, indicating that the mixing of the particles with the two matrices and the coating process do not reduce the antibacterial activity of the plain ZnO particles.

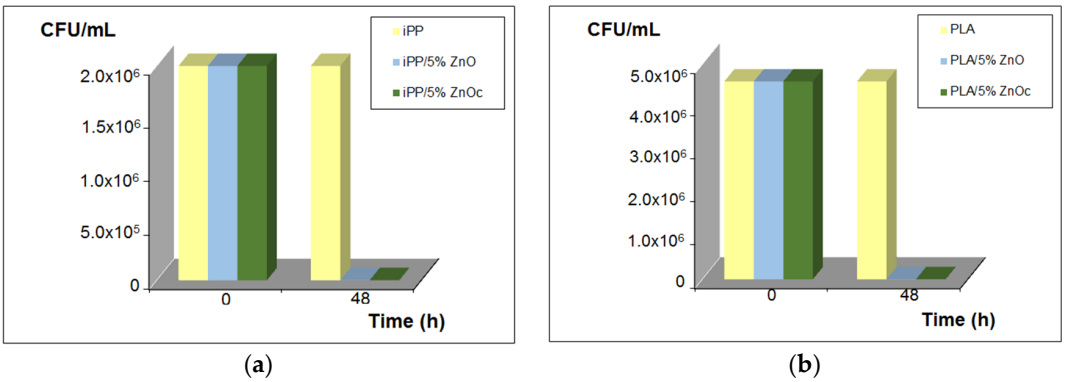

Figure 2. CFU/mL versus contact time for iPP (**a**) and PLA (**b**) based systems.

3.3. Photostability and Thermostability

Figure 3 shows the UV-Visible spectra of iPP and PLA based composites. The two plain polymers, in agreement with literature [10,35], do not have a high photostability (Figure 3). In the case of iPP, UV-Vis analysis shows an absorption band at 280 nm due to the presence of some stabilizer in the commercial iPP used. The PLA transmittance starts to decrease at about 382 nm and becomes 0 at 225 nm, this saturation of the spectra at 225 nm is due to the absorbance of PLA ester groups [9,43].

In the presence of both ZnO and ZnOc for both polymers, an absorption band in the region around 385 nm—as indicated by arrows—is observed [10]. As reported in the literature, this band is due to the inherent capacity of the ZnO particles to absorb the UV light [43,44]. This result indicates that both ZnO and ZnOc particles are able to absorb UV light and to extend the UV absorption area of plain polymers.

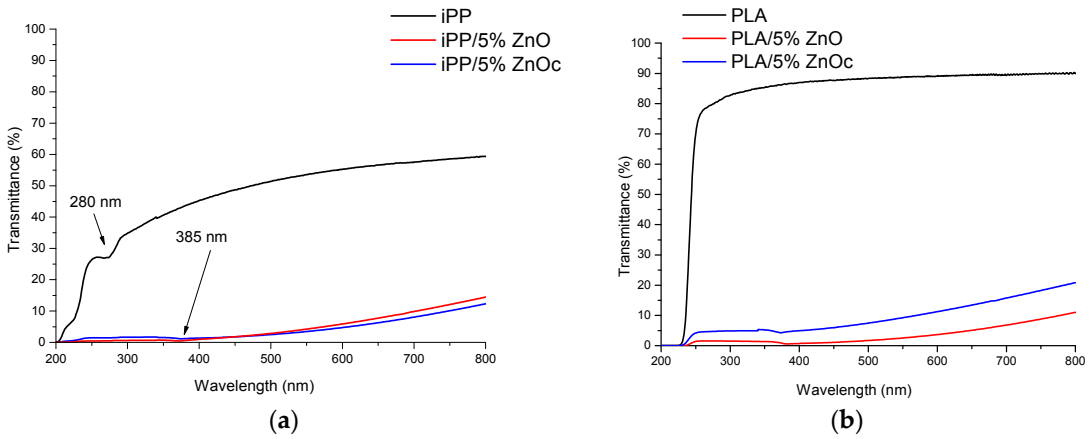

Figure 3. UV-visible spectra of iPP (**a**) and PLA (**b**) based composites.

In Figure 4 the thermostability curves of iPP and PLA based composites are presented. The presence of the ZnO and ZnOc increases or decreases the thermal stability depending on the type of the polymer into consideration. For the iPP/ZnO and iPP/ZnOc systems, there is a delay in the temperature of starting degradation, compared to iPP, and a consistent increase of the temperature at which the weight of the sample is reduced of the 50% ($T_{50\%}$) (see Table 1).

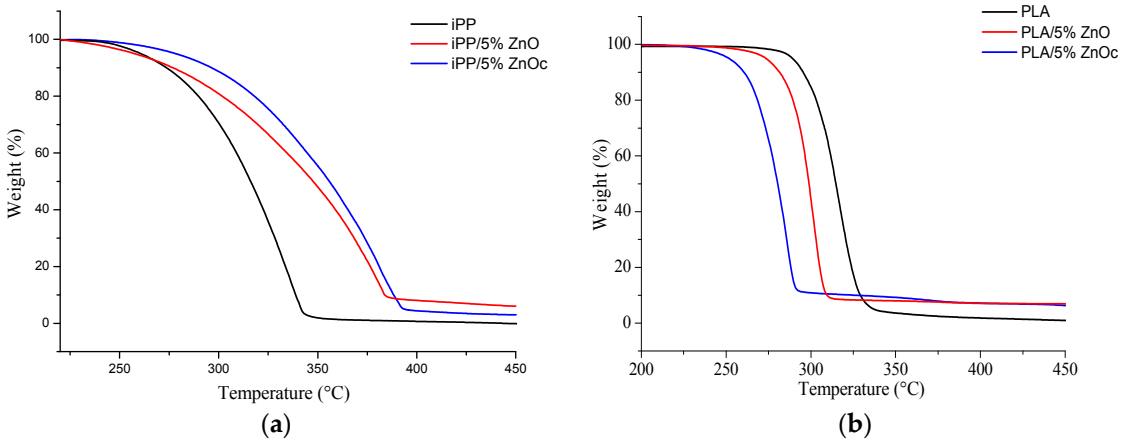

Figure 4. Thermostability curve of iPP (**a**) and PLA (**b**) based composites.

Table 1. Temperature at which the degradation process is at 50%.

Sample	$T_{50\%}$ (°C)
iPP	315 ± 1
iPP/5%ZnO	347 ± 1
iPP/5%ZnOc	355 ± 1
PLA	315 ± 1
PLA/5%ZnO	299 ± 1
PLA/5%ZnOc	280 ± 1

The presence of uncoated ZnO (5 wt %) has consistent influence on the thermostability of iPP, which increases when the ZnO particles are coated by the stearic acid, as seen in Figure 4a. The degradation of the stearic acid, as it was reported in a previous paper [10], starts before the degradation of iPP, acting as a barrier for the degradation of the matrix also slowing the diffusion of the degradation products of iPP in the sample, causing an increase of the thermal stability of iPP/ZnOc.

When the same particles are added to PLA the behavior is completely different, as it is possible to observe in the Figure 4b. Both PLA based composites degrade faster than the plain polymer. Comparing the two composites, the PLA filled with ZnOc degrades faster that the PLA containg the uncoated particles. It is reported in the literature that ZnO particles catalyze the depolymerization [9]. Moreover, these results confirm that the ZnOc increases the PLA degradation process, because of the presence of voids that creates a preferential path for the degradation products to easily leave the sample, and does not permit to the degradation products of the stearic acid to act as a barrier for the degradation of the matrix.

3.4. Mechanical Properties

Figure 5 shows the stress-strain curves of composites, whereas Tables 2 and 3 report the values of mechanical parameters, Young modulus (E), stress and strain at the yield point (σ_y, ε_y), and at break (σ_b, ε_b).

For the iPP based systems, it can be seen that all the samples have the typical behavior of a semi-crystalline polyolefin, with the phenomenon of yield strength, cold drawing, fiber elongation, and final break of the fibers, as seen in Figure 5a. From the values shown in the Table 2, it can be observed that compared with plain iPP the two composite films present improved Young modulus and this improvement is more evident for the system containing the coated particles. These samples present also an improvement in stress at the yield point and comparable values of stress at the break with plain polymer. In conclusion, the sample iPP/ZnOc presents values of mechanical properties higher than those of the iPP/ZnO composite.

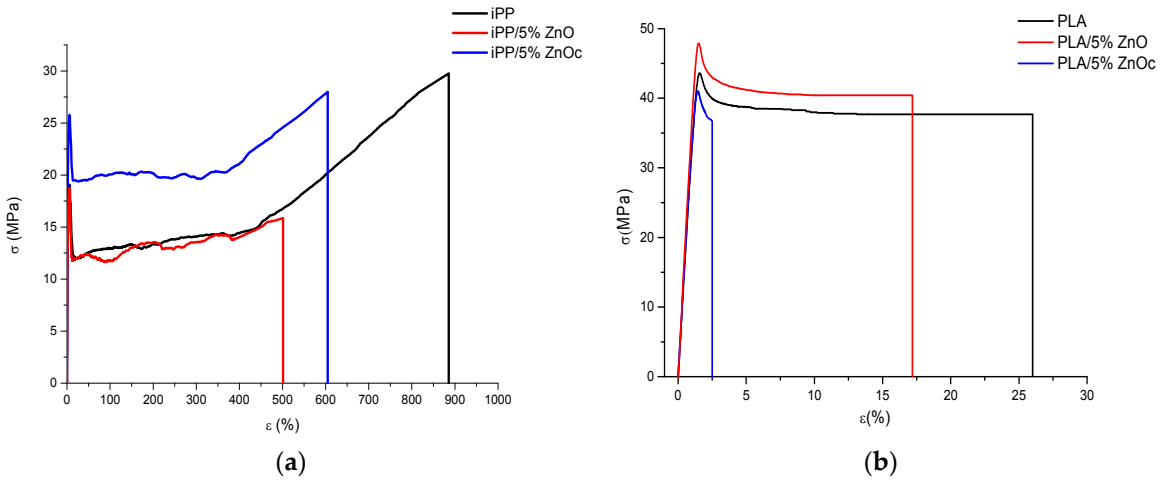

(**a**) (**b**)

Figure 5. Stress-strain curve of iPP (**a**) and PLA (**b**) based systems.

Table 2. Stress–strain parameters of iPP, iPP/5%ZnO, and iPP/5%ZnOc composites.

Sample	E (MPa)	σ_y (MPa)	ε_y (%)	σ_b (MPa)	ε_b (%)
iPP	1350 ± 100	19 ± 3	7 ± 2	30 ± 3	890 ± 65
iPP/5%ZnO	1430 ± 166	19 ± 2	6 ± 1	16 ± 4	500 ± 120
iPP/5%ZnOc	1515 ± 79	26 ± 1	7 ± 1	28 ± 3	605 ± 76

Table 3. Stress–strain parameters of PLA, PLA/5%ZnO, and PLA/5%ZnOc composites.

Samples	*E* (MPa)	σ_y (MPa)	ε_y (%)	σ_b (MPa)	ε_b (%)
PLA	3470 ± 189	44 ± 2	2 ± 1	38 ± 2	26 ± 5
PLA/5%ZnO	3853 ± 107	48 ± 3	2 ± 1	40 ± 3	17 ± 6
PLA/5%ZnOc	3492 ± 184	37 ± 3	3 ± 1	41 ± 3	2 ± 1

Different behavior is found for the PLA based systems. From Figure 5b it is clear that the PLA shows a poor plastic behavior, differently from petroleum-based plastics, however it is possible to observe yielding, drawing, and final rupture of the sample. In particular, it is possible to note, with respect to plain PLA, that when the ZnO particles are present in the PLA matrix there is:

- A slight increase in the modulus and in the stress at the yield point;
- No consistent variation in ε_y and σ_b;
- A decrease in the elongation at the break;
- A strong decrease of the elongation at the break mainly for the PLA/ZnOc system.

The different behavior of the mechanical properties observed in the case of iPP and PLA based systems can be related to the different morphology that is present in the systems. The more homogeneous distribution of the ZnOc particles inside the matrix of iPP causes the improvement in the mechanical properties with respect to the iPP/ZnO system where agglomeration phenomena are present. For the PLA/ZnOc system, not only the agglomeration phenomena, but mainly the poor adhesion between the phases is certainly responsible of the low value of elongation at break, because the fracture can easily propagate through the voids.

3.5. Percentage Variation of Oxygen Permeability

The oxygen permeability of plain iPP is 5.50 $[(cm^3/(m^2 \times 24\ h)] \times (cm/bar)$ and for PLA is 2.23 $[(cm^3/(m^2 \times 24\ h)] \times (cm/bar)$. Table 4 shows the percentage variation of oxygen permeability of the composite films respect the plain iPP and PLA films. For iPP composite films, the permeability is almost the same as that of plain iPP. In the case of PLA based systems, there is a significant decrease of oxygen permeability for PLA/5% ZnO film (18%). With respect to the plain PLA film, this is due to the homogeneous distribution of the ZnO particles in the PLA matrix which makes the path of the oxygen molecules more tortuous [9]; whereas no variation for the PLA system with ZnOc is found.

Table 4. Percentage variation of O_2 permeability of composite systems respect to plain iPP and PLA at 23 °C and 0% HR.

Sample	ΔO_2 Permeability (%)
iPP/5%ZnO	+2%
iPP/5%ZnOc	−3%
PLA/5%ZnO	−18%
PLA/5%ZnOc	+1%

4. Conclusions

The work confirms that the main factors in defining the properties of a composite are the overall morphology (dispersion and distribution of the loads in the polymers matrix), as well as the strength of the adhesion between the matrix and the particles.

In particular, SEM analysis shows homogeneous dispersion and distribution of ZnOc particles in the iPP matrix and of ZnO in the PLA matrix. Consequentially, there is an improvement of the tensile properties for the iPP/ZnOc and PLA/ZnO systems.

It has also to be underlined that the ZnOc particles have a shielding effect to UV radiation as ZnO particles as reported in the literature.

The coated particles influence the thermostability. In particular, when the ZnOc particles are present in the iPP matrix there is an improvement of the thermal stability respect the plain iPP contrary in the PLA matrix. The principal achievements are regarding oxygen permeability where the PLA/ZnO system shows a significant decrease and also about antibacterial activity against *E. coli* where those novel composites show—after 48 h—strong bacterial reduction. This assessment demonstrated that among the reported systems, iPP/5%ZnOc films and PLA/5%ZnO, are the most suitable active materials for potential application in the active packaging field.

Acknowledgments: The authors acknowledge the support from the Eranet Susfood-Cereal "Improved and resource efficiency throughout the post-harvest chain of fresh cut fruits and vegetables", the Erasmus+: "Cooperation and Innovation for Good Practices Joint innovative training and teaching/learning program in enhancing development and transfer knowledge of application of ionizing radiation in materials processing", and the IAEA Coordinated Research P F22063, Italy/Quebec Joint project n. PGR01085.

Author Contributions: Clara Silvestre and Sossio Cimmino supervised the research program. Clara Silvestre, Sossio Cimmino, and Antonella Marra designed the setup. Antonella Marra and Gennaro Rollo performed the experiments. All authors contributed to the analysis of the presented experiments and correlation of the different means of investigations. Antonella Marra and Clara Silvestre wrote the initial draft. Antonella Marra, Clara Silvestre, and Sossio Cimmino coordinated the revisions of the draft in the final form.

Conflicts of Interest: The authors declare no conflict of interest.

References

1. Silvestre, C.; Cimmino, S. *Ecosustainable Polymer Nanomaterials for Food Packaging: Innovative Solutions, Characterization Needs, Safety and Environmental Issues*; Silvestre, C., Cimmino, S., Eds.; CRC Press: Boca Raton, FL, USA, 2013.
2. Sahoo, S. Socio-ethical issues and nanotechnology development: perspectives from India. In Proceedings of 10th IEEE Conference on Nanotechnology (IEEE-NANO), Seoul, Korea, 17–20 August 2010.
3. Sirelkhatim, A.; Mahmud, S.; Seeni, A.; Mohamad, K.N.H.; Ann, L.C.; Bakhori, S.K.M.; Hasan, H.; Mohamad, D. Review on Zinc Oxide Nanoparticles: Antibacterial Activity and Toxicity Mechanism. *Nano-Micro Lett.* **2015**, *7*, 219–242. [CrossRef]
4. Garcia, M.; Forbe, T.; Gonzalez, E. Potential applications of nanotechnology in the agro-food sector. *Cienc. Technol. Aliment.* **2010**, *30*, 573–581. [CrossRef]
5. Ayhan, Z. Potential Applications of Nanotechnology in Food Packaging. In Proceedings of 1st International Congress on Food Technology, Antalya, Turkey, 3–6 November 2010.
6. Duraccio, D.; Silvestre, C.; Cimmino, S.; Marra, A.; Pezzuto, M. *Polymer Morphology: Principles, Characterization, and Processing*; Qi, P.G., Ed.; Wiley: New York, NY, USA, 2016; pp. 374–396.
7. Malucelli, G. Hybrid Organic/Inorganic Coatings through Dual-Cure Processes: State of the Art and Perspectives. *Coatings* **2016**, *6*, 10. [CrossRef]
8. Silvestre, C.; Cimmino, S.; Pezzuto, M.; Marra, A.; Ambrogi, V.; Dexpert-Ghys, J.; Verelst, M.; Augier, S.; Romano, I.; Duraccio, D. Preparation and characterization of isotactic polypropylene/zinc oxide microcomposites with antibacterial activity. *Polym. J.* **2013**, *45*, 938–945. [CrossRef]
9. Marra, A.; Silvestre, C.; Duraccio, D.; Cimmino, S. Polylactic Acid/Zinc Oxide biocomposite films for food packaging application. *Int. J. Biol. Macromol.* **2016**, *88*, 254–262. [CrossRef] [PubMed]
10. Silvestre, C.; Duraccio, D.; Marra, A.; Strongone, V.; Cimmino, S. Development of Antibacterial Composite Films Based on Isotactic Polypropylene and Coated ZnO Particles for Active Food Packaging. *Coatings* **2016**, *6*, 4. [CrossRef]
11. Duncan, T.V. Applications of nanotechnology in food packaging and food safety: Barrier materials, antimicrobials and sensors. *J. Colloid Interface Sci.* **2011**, *363*, 1–24. [CrossRef] [PubMed]
12. Mihindukulasuriya, S.D.F.; Lim, L.T. Nanotechnology development in food packaging: A review. *Trends Food Sci. Technol.* **2014**, *40*, 149–167. [CrossRef]
13. Reuge, N.; Caussat, B.; Joffin, N.; Dexpert-Ghys, J.; Verelst, M.; Dxpert, H. Modelling of Spray Pyrolysis-Why the Synthesized Y_2O_3 Microparticles hollow. *AlChE J.* **2008**, *54*, 394–405. [CrossRef]
14. Rossignol, C.; Verelst, M.; Dexpert-Ghys, J.; Rul, S. Synthesis of undoped ZnO nanoparticles by spray pyrolysis. *Adv. Sci. Thecnol.* **2006**, *45*, 237–241. [CrossRef]

15. Caiut, J.M.A.; Dexpert-Ghys, J.; Kihn, Y.; Veelst, M.; Dexpert, H.; Ribeiro, S.J.L.; Messaddeq, Y. Elaboration of boehmite nano-powders by spray-pyrolisis. *Powder Thecnol.* **2009**, *190*, 95–98. [CrossRef]
16. Bacsa, R.; Kihn, Y.; Verelst, M.; Dexpert-Ghys, J.; Bacsa, W.; Serp, P. Large scale synthesis of zinc oxide nanorods by homogeneous chemical vapour deposition and their characterization. *Surf. Coat. Technol.* **2007**, *201*, 9200–9204. [CrossRef]
17. Zhou, N.; Liu, Y.; Li, L.; Meng, N.; Huang, Y.; Zhang, J.; Wei, S.; Shen, J. A new nanocomposite biomedical material of polymer. *Curr. Appl. Phys.* **2007**, *7*, 58–62. [CrossRef]
18. Seyfriedsberger, G.; Rametsteine, K.; Kern, W. Polyethylene compounds with antimicrobial surface properties. *Eur. Polym. J.* **2006**, *42*, 3383–3389. [CrossRef]
19. Kumar, R.; Münstedt, H. Silver ion release from antimicrobial polyamide/silver composites. *Biomaterials* **2005**, *26*, 2081–2088. [CrossRef] [PubMed]
20. Soriano, C.B.; Martínez, V.P.; López, A.M.C.; Ortega, B.I.; Grande, B.M.J.; Pérez, P.R.; Gálvez, A.; Lucas, L.R. Effect of Activated Plastic Films on Inactivation of Foodborne Pathogens. *Coatings* **2016**, *6*, 28. [CrossRef]
21. Silvestre, C.; Duraccio, D.; Cimmino, S. Food packaging based on polymer nanomaterials. *Prog. Polym. Sci.* **2011**, *36*, 1766–1782. [CrossRef]
22. Liau, S.Y.; Read, D.C.; Pugh, W.; Furr, J.R.; Russell, A.D. Interaction of silver nitrate with readily identifiable groups: Relationship to the antibacterial action of silver ions. *Lett. Appl. Microbiol.* **1997**, *25*, 279–283. [CrossRef] [PubMed]
23. Fujishima, A.; Rao, T.N.; Tryk, D.A. Titanium dioxide photocatalysis. *Photochem. Photobiol. C* **2000**, *1*, 1–21. [CrossRef]
24. Santhosh, S.M.; Natarajan, K. Antibiofilm Activity of Epoxy/Ag-TiO_2 Polymer Nanocomposite Coatings against Staphylococcus Aureus and *Escherichia Coli*. *Coatings* **2015**, *5*, 95–114.
25. Santos, G.N.C.; Tibayan, E.B.; Castillon, G.B.; Estacio, E.; Furuya, T.; Iwamae, A.; Yamamoto, K.; Tani, M. Tin Oxide-Silver Composite Nanomaterial Coating for UV Protection and Its Bactericidal Effect on *Escherichia coli* (*E. coli*). *Coatings* **2014**, *4*, 320–328. [CrossRef]
26. Jones, N.; Ray, B.; Ranjit, K.T.; Manna, A.C. Antibacterial activity of ZnO nanoparticle suspensions on a broad spectrum of microorganisms. *FEMS Microbiol. Lett.* **2008**, *279*, 71–76. [CrossRef] [PubMed]
27. Sawai, J.; Yoshikawa, T.J. Quantitative evaluation of antifungal activity of metallic oxide powders (MgO, CaO and ZnO) by an indirect conductimetric assay. *Appl. Microbiol.* **2004**, *96*, 803–809. [CrossRef]
28. Yamamoto, O.; Nakakoshi, K.; Sasamoto, T.; Nakagawa, H.; Miura, K. Adsorption and growth inhibition of bacteria on carbon materials containing zinc oxide. *Carbon* **2001**, *39*, 1643–1651. [CrossRef]
29. Brayner, R.; Ferrari-lliou, R.; Brivois, N.; Djediat, S.; Benedetti, M.F.; Fiévet, F. Toxicological Impact Studies Based on Escherichia coli Bacteria in Ultrafine ZnO Nanoparticles Colloidal Medium. *Nano Lett.* **2006**, *6*, 866–870. [CrossRef] [PubMed]
30. Yamamoto, O.; Komatsu, M.; Sawai, J.; Nakagawa, Z. Effect of lattice constant of zinc oxide on antibacterial characteristics. *J. Mater. Sci. Mater.* **2004**, *15*, 847–851. [CrossRef] [PubMed]
31. Stoimenov, P.K.; Klinger, R.L.; Marchin, G.L.; Klabunde, K.J. Metal Oxide Nanoparticles as Bactericidal Agents. *Langmuir* **2002**, *18*, 6679–6686. [CrossRef]
32. Tam, K.H.; Djurišic, A.B.; Chan, C.M.N.; Xi, Y.Y.; Tse, C.W.; Leung, Y.H.; Chan, W.K.; Leung, F.C.C.; Au, D.W.T. Antibacterial activity of ZnO nanorods prepared by a hydrothermal method. *Thin Solid Films* **2008**, *516*, 6167–6174. [CrossRef]
33. Espitia, P.J.P.; Soares, N.F.F.; Coimbra, J.S.R.; de Andrade, N.J.; Cruz, R.S.; Medeiros, E.A. A Zinc Oxide Nanoparticles: Synthesis, Antimicrobial Activity and Food Packaging Applications. *Food Bioprocess Technol.* **2012**, *5*, 1447–1464. [CrossRef]
34. Martínez-Bueno, M.J.; Cimmino, S.; Silvestre, C.; Tadeo, J.L.; Garcia-Valcárcel, A.I.; Fernández-Alba, A.R.; Hernando, M.D. Characterization of non-intentionally added substances (NIAS) and zinc oxide nanoparticle release from evaluation of new antimicrobial food contact materials by both LC-QTOF-MS, GC-QTOF-MS and ICP-MS. *Anal. Methods* **2016**, *8*, 7209–7216. [CrossRef]
35. Marra, A.; Boumail, A.; Cimmino, S.; Criado, P.; Silvestre, C.; Lacroix, M. Effect of PLA/ZnO Packaging and Gamma Radiation on the Content of Listeria innocua, Escherichia coli and Salmonella enterica on Ham during Storage at 4 °C. *J. Food Sci. Eng.* **2016**, *6*, 245–259.

36. Salvatore, M.; Marra, A.; Duraccio, D.; Shayanfar, S.; Pillai, S.D.; Cimmino, S.; Silvestre, C. Effect of electron beam irradiation on the properties of polylactic acid/montmorillonite nanocomposites for food packaging applications. *J. Appl. Polym. Sci.* **2016**, *133*, 42219. [CrossRef]
37. Weber, C.J.; Haugaard, V.; Festersen, R.; Bertelsen, G. Production and applications of biobased packaging materials for the food industry. *J. Food Addit. Contam.* **2002**, *19*, 172–177. [CrossRef] [PubMed]
38. Gurav, A.; Kodas, T.; Pluym, T.; Xiong, Y. Aerosol processing of materials. *Aerosol Sci. Technol.* **1993**, *19*, 411–452. [CrossRef]
39. Pratsinis, S.E.; Vemury, S. Particle formation in gases. *Powder Technol.* **1996**, *88*, 267–273. [CrossRef]
40. Messing, G.L.; Zhang, S.C.; Jayanthi, G.V. Ceramic powder synthesis by spray pyrolysis. *J. Am. Ceram. Soc.* **1993**, *76*, 2707–2726. [CrossRef]
41. Alavi, S.; Caussat, B.; Couderc, J.P.; Dexpert-Ghys, J.; Joffin, N.; Neumeyer, D.; Verelst, M. Spray pyrolysis synthesis of submicronic particles. Possibilities and limits. *Adv. Sci. Technol. A* **2003**, *30*, 417–424.
42. *ASTM E2149-10 Standard Test Method for Determining the Antimicrobial Activity of Immobilized Antimicrobial Agents Under Dynamic Contact Conditions*; ASTM International: West Conshohocken, PA, USA, 2010.
43. Bocchini, S.; Fukushima, K.; Di Blasio, A.; Fina, A.; Frache, A.; Geobaldo, F. Polylactic Acid and Polylactic Acid-Based Nanocomposite Photooxidation. *Biomacromolecules* **2010**, *11*, 2919–2926. [CrossRef] [PubMed]
44. Utracki, L.A. Compatibilization of polymer blends. *Can. J. Chem. Eng.* **2002**, *80*, 1008–1016. [CrossRef]